Reduction of nitrite to NO in an organised triphasic medium by platinum carbonyl clusters and redox active dyes as electron carriers†

Nalinava Sen Gupta,[a] Susmit Basu,[a] Pramatha Payra,[a] Pradeep Mathur,[a] Sumit Bhaduri*[b] and Goutam Kumar Lahiri*[a]

Received 5th March 2007, Accepted 29th March 2007
First published as an Advance Article on the web 19th April 2007
DOI: 10.1039/b703352d

Artificial electron donors such as *leuco* methylene blue and *leuco* safranin O reduce nitrite ion to nitric oxide. The reaction is effected in a U-tube where nitrite ion and dye in two aqueous layers are separated by a layer of dichloromethane (a close model for a biological liquid membrane) that contains the platinum carbonyl cluster ($[Bu_4N]_2[Pt_{12}(CO)_{24}]$, Chini cluster). On passing dihydrogen an electron transfer chain involving dihydrogen, the dye, the clusters and the nitrite ion is initiated. The cluster catalytically reduces the dye in the presence of dihydrogen, the reduced dye migrates across the phase boundaries and in turn reduces the nitrite ions. The resultant nitric oxide in the effluent gas has been identified by its reactions with cobalamine and myoglobin. When safranin O is the dye, an adduct is formed between the reduced dye and NO. It has been identified by spectroscopic techniques and its probable structure investigated by DFT calculations.

Introduction

Reductions of nitrite in biological processes such as denitrification and meat curing have been known for a long time. However, the ability of nitrite as a major bio-available pool of NO and to intervene in blood flow regulation by reaction with deoxygenated hemoglobin (Hb) has only recently come to light.[1–3] A recent report also shows that in the presence of nitrite, the enzyme xanthine oxidoreductase plays a protective role by reducing nitrite to NO.[4] In view of these reports, the design of chemical models for the biological reduction of nitrite to nitric oxide is important.

To a first approximation, any chemical model for a biological redox reaction such as eqn (1), should satisfy the following conditions. As most biological redox reactions involve an electron

$$NO_2^- + 2H^+ + e^- \rightarrow NO + H_2O \quad (1)$$

transfer chain and more than one electron carrier, *i.e.* a redox catalyst, the model reaction should mimic this feature. Second, the specific carrier that transfers the electron to nitrite must be active as an artificial electron donor/acceptor in an actual biological system. Third, while the electron and proton transfer to nitrite may take place in an aqueous medium, the electron transport chain like that in mitochondria, must operate across a model membrane. Finally, in the model, if there is an *in situ* formation of an "A–NO" bond (A = S or N) from the liberated NO and the electron carrier, it would be an additional attractive feature. This is because while thionitrosyls (RSNO) have been intensively studied as the major carriers of NO, recently it has been shown that *N*-nitrosation and heme-nitrosylation are also as ubiquitous as *S*-nitrosation.[5,6]

The work reported here was undertaken with two objectives. First, to construct a model that satisfies all the four conditions mentioned above. Second to find out if artificial electron donors such as *leuco* methylene blue (MBH) or *leuco* safranin O (SafH) could reduce NO_2^- to NO. The use of these redox active dyes as artificial electron acceptors and/or donors is well established in biochemical and biological research.[7] In our previous publications we have shown, that the reduction of a chemical analogue of biological NAD^+ by SafH, is chemo- and regio-selective.[8] Also by using catalytic amounts of Saf^+, NAD^+, $[Pt_{12}(CO)_{24}]^{2-}$ and the enzyme lactate dehydrogenase, the enantioselective hydrogenation of methyl pyruvate to methyl lactate by dihydrogen in a biphasic system could be achieved.[9] We have also shown that in a triphasic system (two aqueous layers separated by an organic layer), $[Pt_{12}(CO)_{24}]^{2-}$, due to its unique redox properties can mimic the pH driven electron transport of biological systems.[10]

The model described in this paper utilises the results and insights gained from our early work. Here we have used a U-tube (Fig. 1) where an aqueous solution of nitrite and an aqueous solution of the artificial electron carrier are separated by a water immiscible organic liquid such as dichloromethane. This type of triphasic system in a U-tube has been used in the past to model the gross features of a biological membrane that separates out the inner and outer aqueous phases of a cell. However, to the best of our knowledge there have been no reports on the use of such models for biological redox reactions in general and nitrite reductions in particular. The NO produced by the reduction of the nitrite ion in turn reacts with SafH to give SafH–NO. This adduct SafH–NO has a "N–NO" linkage, is stable enough to be characterised by spectroscopic techniques. No such adduct formation is observed with MBH. This difference in behaviour between SafH and MBH has been rationalised by DFT calculations.

[a]*Department of Chemistry, Indian Institute of Technology-Bombay, Powai, Mumbai, 400076, India. E-mail: lahiri@chem.iitb.ac.in; Fax: +91 22 25763480; Tel: +91 22 25767159*
[b]*Reliance Industries Limited, Swastik Mills Compound, V.N. Purav Marg, Chembur, Mumbai, 400071, India. E-mail: sumit_bhaduri@ril.com; Fax: +91 22 67677380; Tel: +91 22 67677324*

† Electronic supplementary information (ESI) available: ESR (Fig. S1) and IR (Fig. S2) spectra of [Co(Salen)]/[(NO)Co(Salen)]; UV-Visible spectral changes of nitrite reduction to NO by SafH (Fig. S3).

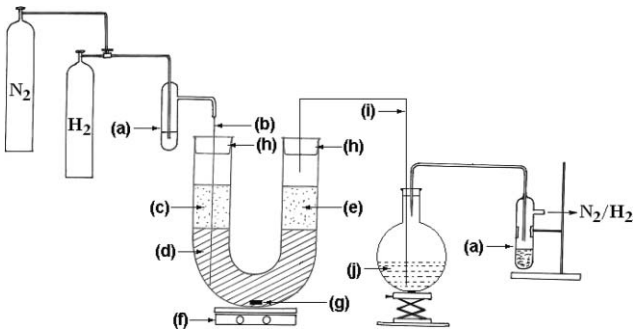

Fig. 1 U-tube reaction setup for the reduction of nitrite and subsequent trapping of the effluent gas. The whole setup was degassed by purging nitrogen prior to start the reaction. (a) oil bubbler, (b) inlet needle, (c) aqueous layer containing $NaNO_2$ solution, (d) dichloromethane layer containing catalyst $[Bu_4N]_2[Pt_{12}(CO)_{24}]$, (e) aqueous layer containing dye solution, (f) magnetic stirrer, (g) magnetic bar, (h) rubber septum, (i) outlet needle (vent), (j) solution of trapping agent for the effluent NO gas through the vent.

Results and discussion

The model arrangement (U-tube set up, Fig. 1) for the reduction of nitrite to nitric oxide described here consists of two aqueous phases, one containing nitrite and the other containing the oxidised dye (Dye_{ox} = Saf^+ or MB^+). The two aqueous layers are separated by a layer of dichloromethane that contains $[Bu_4N]_2[Pt_{12}(CO)_{24}]$, **1**, which is insoluble in water but soluble in dichloromethane. The rationale behind using a triphasic rather than a bipasic system is as follows. Separating out the nitrite layer from that of the Dye_{ox} ensures that there is minimum interference from organic species during spectrophotometric monitoring of the left hand side aqueous layer and also quantitative turnover number measurements by IR (see later).

By a control experiment it was first established that in the absence of Dye_{ox}, **1** by itself could not reduce nitrite ions. Under these conditions the literature reported reduction of $[Pt_{12}(CO)_{24}]^{2-}$ to $[Pt_9(CO)_{18}]^{2-}$ *i.e.*, eqn (2), does occur but there is no observable reduction

$$3[Pt_{12}(CO)_{24}]^{2-} + H_2 \rightarrow 4[Pt_9(CO)_{18}]^{2-} + 2H^+ \quad (2)$$

of nitrite. In the presence of Dye_{ox} in the right hand side aqueous layer, selective reduction of Dye_{ox} to Dye_{red} (Dye_{red} = SafH and MBH) by dihydrogen and catalysed by **1**, is observed.[8,9] As indicated in Scheme 1 both Dye_{ox} and Dye_{red} have measurable solubilities in water and dichloromethane, and the partition coefficients of Saf^+ and SafH in a 1 : 1 mixture of water and dichloromethane are 6.8 and 0.14, respectively.[10] Thus the solubility of Dye_{red} in both organic and aqueous media enables it to act as a shuttle carrier, and to transfer the required redox equivalents across the phase boundary (Scheme 1).

The ability of **1** to act as a selective redox catalyst for the reduction of Dye_{ox} is due to reactions as stated in eqn (2) and (3) and slight solubility of Dye_{ox} in dichloromethane.[9–12]

$$4[Pt_9(CO)_{18}]^{2-} + Dye_{ox} + H^+ \rightarrow 3[Pt_{12}(CO)_{24}]^{2-} + Dye_{red} \quad (3)$$

Combination of these two reactions gives the overall reaction, eqn (4), and on passing hydrogen through the dichloromethane layer, the electron transfer chains shown in Scheme 1 are initiated.

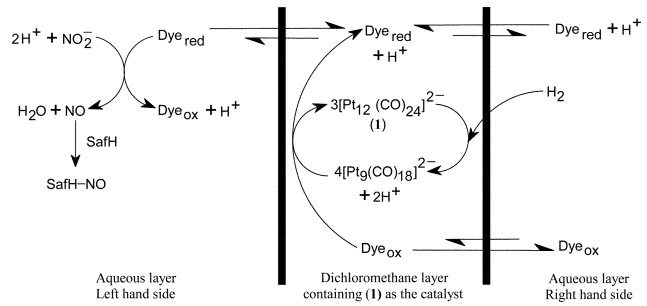

Scheme 1 Reduction of nitrite by Dye_{red} in a U-tube. **1** catalyses the reduction of Dye_{ox} to Dye_{red} by dihydrogen. The comparative lengths of the half arrows in the equilibria are indicative of the solubilities of Dye_{ox}/Dye_{red} in dichloromethane and water.

The reduction of Dye_{ox} is rapid, but the reduction of nitrite to NO in the other aqueous layer, *i.e.*

$$Dye_{ox} + H_2 \rightarrow Dye_{red} + H^+ \quad (4)$$

eqn (5), commences only after an induction time. The induction time depends on the rate of

$$Dye_{red} + H^+ + 2NO_2^- \rightarrow Dye_{ox} + 2NO + 2HO^- \quad (5)$$

stirring and hydrogen bubbling, *i.e.* the rate of diffusion of Dye_{red} across the two phase boundaries. It may be noted that combination of eqn (4) and (5) gives eqn (6), which is the net catalytic reaction. This reaction is thermodynamically slightly unfavourable and in the absence of catalysts it does not take place.

$$H_2 + 2NO_2^- \rightarrow 2NO + 2HO^- \quad (6)$$

All the reactions have been carried out at neutral pH and no attempt was made to study the effect of pH on the overall reaction. This is because the carbonyl clusters undergo facile reactions with H^+ and HO^-. From a practical point of view this limits the productive use of the catalytic system for any denitrification reaction. Furthermore, apart from the reactions shown in Scheme 1 more complex reactions are possible and indeed do take place when the model is operated for a long ($\geq$ 3 h) time. Under these conditions the evolved nitric oxide reacts with the carbonyl clusters and produces complexes with spectral signatures different from that of the original clusters. No attempt was made to identify these complexes.

During the induction time spectroscopic monitoring shows no change in the nitrite solution, but in the dichloromethane and the Dye_{ox} aqueous layers, changes are consistent with reactions in eqn (2)–(4). The formation of NO commences after the induction time, and its presence in the effluent hydrogen is evidenced by its reactions separately with Co(Salen) [Salen = *N*,*N*′-ethylenebis(salicylideneiminato)], cobalamine/glutathione and also myoglobin. It is important to note that the overall electron transfer chain that ends with the reduction of nitrite, critically depends on the selective reduction of Dye_{ox} to Dye_{red} and therefore cannot be achieved by conventional heterogeneous catalysts such as platinum on carbon which over reduces and/or decomposes Dye_{ox}.[9]

The black crystalline product isolated from the reaction of the effluent gas with Co(Salen) is identified as [Co(Salen)(NO)] on the basis of analytical data and spectroscopic comparison with an authentic sample (Fig. S1 and S2†).[13] The reaction of NO with

cobalamine in the presence of glutathione (GSH) is known to exhibit characteristic spectrophotometric changes.[14] In our system too, the effluent gas on reaction with cobalamine and glutathione, brings about all the essential features of the literature reported spectrophotometric changes (Fig. 2). Thus isobestic points close to 500, 400 and 300 nm are observed and while the absorption above 500 nm decreases in intensity, there is a gradual increase in the intensity in absorption between 400–500 nm. The reaction of myoglobin (Mb) with NO has recently been much studied.[15] On passing the effluent gas through a freshly prepared solution of Mb, the characteristic band of Mb–NO is also observed (Fig. 3).

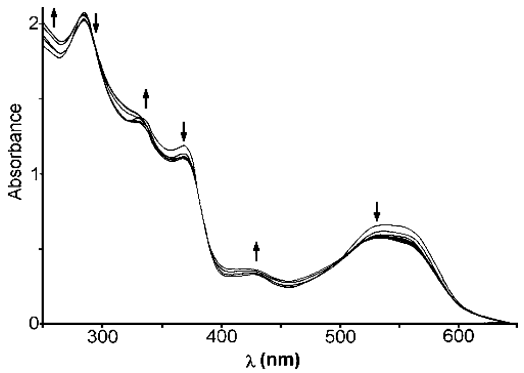

Fig. 2 Changes in the UV-Visible spectra on passing the effluent gas through a GS–Cbl(III) solution in water.

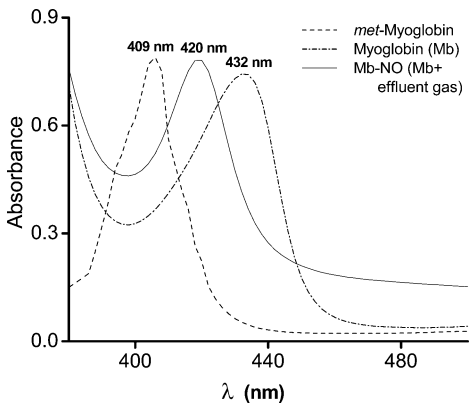

Fig. 3 Changes in the UV-Visible spectra on passing the effluent gas through a freshly prepared myoglobin solution in water.

The turnover numbers for the reduction of NO_2^- to NO for Saf^+ and MB^+ over a period of one hour are 18 ± 2 and 10 ± 2, respectively. During the induction time, isobesticities corresponding to the conversion of Saf^+ to SafH is observed by spectrophotometry (Fig. S3†). However, at the end of the induction time the commencement of NO formation is found to be accompanied by the loss of isobesticity, and the formation of an absorbing species that is ESR active. At the end of an experimental run trace quantities of a dichloromethane soluble solid could be extracted from the nitrite layer. This solid shows an IR band at 1428 cm^{-1} (Fig. 4) assignable to the N–NO linkage, an ESR signal at g ~2.0 (77 K) (Fig. 5) and a molecular ion peak at 346.166 (m/z) (Fig. 6, the peaks for dicationic $[MH]^{2+}$ and tricationic $[MH_2]^{3+}$ species are also observed at 173.586 and 116.060, respectively). As the amount of material formed was exceedingly small (< 0.5 mg), no attempts were made for microanalysis or yield measurements. However, the spectroscopic observations taken together convincingly suggest its formulation to be SafH–NO. In contrast to the case of MB^+, the organic solid which extracted from the nitrite layer has been identified spectroscopically as simply MB^+.

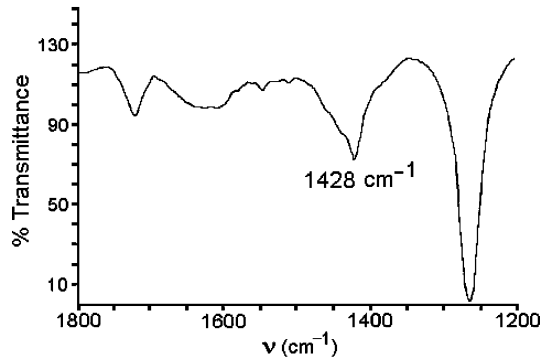

Fig. 4 IR spectrum (in $CHCl_3$) of SafHNO. The peak at 1428 cm^{-1} corresponds to *N*-nitroso (N–N=O) functionality.

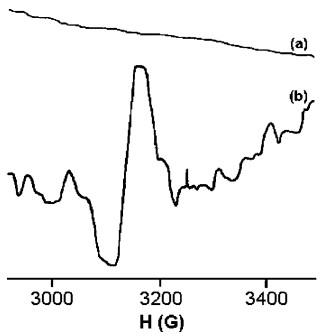

Fig. 5 ESR spectrum (in CH_2Cl_2 at 77 K) of (a) before passing the effluent gas in Saf^+Cl^-, (b) after passing the effluent gas coming out from the vent into Saf^+Cl^-.

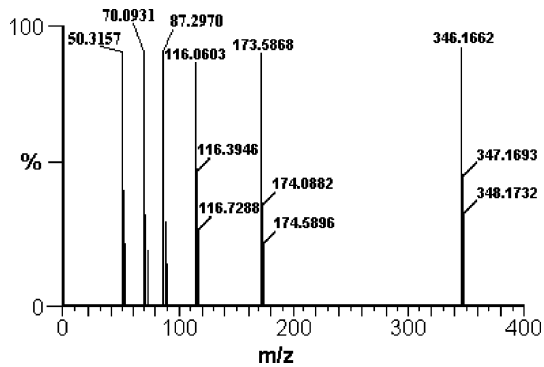

Fig. 6 Electrospray mass spectrum of SafHNO (in methanol). The peak at 346.166 authenticates the formation of SafHNO. The peaks at 173.586 and 116.060 correspond to dicationic $[MH]^{2+}$ and tricationic $[MH_2]^{3+}$ species, respectively

To provide a rationale for the difference in reactivity between MBH and SafH towards NO, and the stability of SafH–NO that allows its isolation to be possible, DFT (B3LYP/6-31G*)

Table 1 Zero point energy (ZPE) corrected relative energies (kcal mol^{-1}) of optimised MBHNO and SafHNO adducts at B3LYP/6–31G* level and corresponding "N–NO" bond lengths[a]

Adducts	E_{stabl}[b]/kcal mol^{-1}	Bond length of N–NO/Å
MBH–NO (^{1}N)	−1.25	2.692
MBH–NO (^{2}N)	−1.48	2.736
MBH–NO (S)	−0.66	3.164
SafH–NO (^{2}N)	−3.03	2.538
SafH–NO (^{3}N)	−1.12	2.954
SafH–NO (^{1}N)	−1.88	2.675

[a] Total ZPE corrected energies (electronic + ZPE in a.u.) calculated at B3LYP/6–31G* level of MBH, SafH and NO are: MBH = −1261.822356; SafH = −992.825202; NO = −129.883621. The atom to which NO binds is given in parentheses and Scheme 2. [b] E_{stabl} is relative stabilization energy ($E_{stabl} = E$(Adduct) − [E(MBH/SafH) + E(NO)]) in kcal mol^{-1}.

calculations have been carried out. Six possible structures, three for each dye, with "N–NO" and "S–NO" (for MBH) linkages have been considered. The relative stabilisation energies of Dye_{red}–NO with respect to the total energy of Dye_{red} and NO, are given in Table 1. From the data it is observed that for both the dyes the adducts with NO linked to the ring 'NH' *i.e.*, N(2), are the most stabilised (Scheme 2).

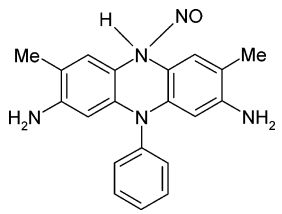

Scheme 2 Most stable structures of SafH–NO according to DFT (B3LYP/6–31G*) calculations.

Furthermore, the SafH–NO adduct is about 1.2 kcal mol^{-1} more stable than the MBH–NO adduct and has the shortest 'N–N' bond length. The calculation results are thus consistent with the observed stability of SafH–NO. Among the MBH–NO adducts, the one with NO linked to the sulfur atom is the least stabilised. This is not surprising since in MBH the sulfur atom is sp^2 hybridised, but biological NO carriers that have thionitrosyl functionalities, have an sp^3 hybridised sulfur atom. It should be noted that the DFT methods at this basis set are not expected to provide an accurate quantitative measure of the stabilities of the adducts. However they are sensitive enough to predict the *trend* in the relative stabilities of the adducts. Our future work will be directed towards providing experimental evidence for the structure shown above.

Conclusions

In conclusion, the present article demonstrates the design of a unique liquid triphasic chemical model close to the liquid membrane based biologically relevant catalytic reduction of nitrite to NO in the presence of electron carriers, $[Pt_{12}(CO)_{24}]^{2-}$/$[Pt_9(CO)_{18}]^{2-}$ and dyes (safranin O/methylene blue).

Experimental

General

All reactions and manipulations were performed under an inert atmosphere. Solvents were dried, distilled and degassed appropriately. For taking out aliquots from the aqueous layer maintaining an inert atmosphere, a cannula technique was used. An argon flow throughout the system and a vacuum inside the cuvette were applied to transfer the part of the aqueous layer through the cannula into the cuvette. Sodium nitrite, safranin O, methylene blue, tetra-n-butylammonium bromide, met-myoglobin, were obtained from Sigma-Aldrich. Hexachloroplatinic acid was obtained from Johnson-Mathey. Cobalamine and glutathione were purchased from Fluka and Lancaster, respectively. Salicylaldehyde, ethylenediamine, sodium acetate, cobalt(II) chloride, ethanol and chloroform were purchased from SDfine Chemicals (India). Other solvents were obtained from Merck. The platinum carbonyl cluster $[Bu_4N]_2[Pt_{12}(CO)_{24}]$ was prepared according to the literature reported procedure.[11] Double distilled deionised water of pH ~6.5 was used for preparing the nitrite solution.

Infrared spectra were recorded on a Nicolet Impact 400 FTIR spectrophotometer, as solutions in a 0.1 mm path length and CsCl disks for Nujol mull and KBr pellets for solid state according to the purpose. ESR spectra were monitored with a Varian model and calibrated by using the tetracyanoethylene radical ($g = 2.0023$). Mass spectra were taken in a Q-TOF (YA-105) micro mass spectrometer. UV-Visible spectra were recorded on a Perkin Elmer Lambda 950 spectrophotometer.

Experimental set up for nitrite reduction

For the reduction of nitrite, the U-tube reaction set up was used (Fig. 1). The catalyst ($[Bu_4N]_2[Pt_{12}(CO)_{24}]$, 0.1 g, 0.0285 mmol) was dissolved in an organic layer (25 cm^3 of dichloromethane). An aqueous solution (15 cm^3) of sodium nitrite (0.1 g, 1.449 mmol) was kept in one arm and in the other arm a safranin O (0.002 g, 0.0056 mmol) solution (15 cm^3) was kept. The ratio of safranin O to cluster (~0.2) was deliberately kept at a low level to avoid interference by the dye in spectroscopic measurements. The two aqueous layers were separated by the organic layer containing catalyst solution in dichloromethane. Both the openings of the U-tube arms were capped with rubber septums. During the course of the reaction dihydrogen gas was bubbled through the dichloromethane solution using a needle without allowing any mixing between the two aqueous layers. The organic layer was stirred vigorously with a magnetic stirrer.

The nitrite reduction reaction using a U-tube set up was monitored by IR spectroscopy using sodium acetate as an internal standard. The change in concentration of NO_2^- in the aqueous layer was determined by following the change in ratio of IR peak areas (the area under the peak was calculated by measuring the half width and the height of the IR peak) of internal standard acetate ($\nu_{acetate} = 1644$ cm^{-1}) and nitrite ($\nu_{nitrite} = 1271$ cm^{-1}).

Identification of NO in the effluent gas

The effluent gas coming out from the vent (Fig. 1) was passed through a cannula to a chloroform solution of Co(Salen).

The black crystalline compound *N*,*N*′-ethylenebis(salicylideneiminato)nitrosylcobalt [(NO)Co(Salen)] was obtained and its ESR (Fig. S1†) and IR (Fig. S2†) spectra were compared with those of an authentic sample.

In a separate reaction the effluent gas coming out from the vent was passed through a cannula into a freshly prepared aqueous solution of glutathione–cobalamine (0.4 mmol cobalamine and 4 mmol glutathione were mixed in 20 cm^3 distilled water and phosphate buffer was used to make the solution of pH = 7). A colour change from violet to brown was observed indicating the cobalamine–NO adduct formation which was further followed by UV-Visible spectral changes (Fig. 2).

Similarly the effluent gas coming out from the vent was also passed through a cannula to a freshly prepared aqueous solution of myoglobin (Mb). The formation of the Mb–NO adduct was confirmed by UV-Visible spectroscopy (Fig. 3).

Spectroscopic identification of SafH–NO

The reduction of nitrite in the U-tube was carried out as mentioned above and the UV-Visible spectra of both the aqueous layers were monitored (Fig. S3†). For isolation of the solid after 120 min reaction the left hand aqueous phase was taken to dryness, the solid residue extracted with dichloromethane and the dichloromethane layer taken to dryness to give a very small amount (< 0.5 mg) of an orange solid. The IR ($CHCl_3$), ESR (CH_2Cl_2, 77 K) and mass spectrum (in methanol, ion-spray) and of this solid were recorded and shown in Fig. 4, 5 and 6, respectively.

Methodology for the DFT calculations

The optimized geometries of all the MBH, SafH and their corresponding NO adducts have been obtained by using the hybrid density functional method (B3LYP)[16] (three parameter Becke's exchange energy functional along with correlational functional due to Lee, Yang and Parr). Specifically, for the closed shell geometries of MBH and SafH, the B3LYP method has been used and for all open shell geometries of free NO and all MBH–NO and SafH–NO adducts, the UB3LYP method (unrestricted open shell calculations) has been utilized. The basis set used in these calculations is 6–31G* in which all core electrons have been explicitly considered. The vibrational frequencies and zero point corrected energies (ZPE) of all the optimized structures have been obtained. All the calculations have been performed using the program Gaussian 98.[17]

Acknowledgements

Financial support received from Reliance Industries Limited, Mumbai, India is gratefully acknowledged. We thank Dr S. Mukhopadhyay and Dr S. Kulkarni (Vlife Sciences Technologies Pvt. Ltd., Pune, India) for their contributions to the DFT calculations.

References

1 (*a*) B. A. Averill, *Chem. Rev.*, 1996, **96**, 2951; (*b*) I. M. Wasser, S. de Vries, P. Moënne-Loccoz, I. Schröder and K. D. Karlin, *Chem. Rev.*, 2002, **102**, 1201.
2 M. T. Gladwin, *J. Clin. Invest.*, 2004, **113**, 19.
3 (*a*) K. Cosby, K. S. Partovi, J. H. Crawford, R. P. Patel, C. D. Reiter, S. Martyr, B. K. Yang, M. A. Waclawiw, G. Zalos, X. Xu, K. T. Huang, H. Shields, D. B. Kim-Shapiro, A. N. Schechter, R. O. Cannon and M. T. Gladwin, *Nat. Med.*, 2003, **12**, 1498 and references therein; (*b*) S. Shiva, X. Wang, L. A. Ringwood, X. Xu, S. Yuditskaya, V. Annavajjhala, H. Miyajima, N. Hogg, Z. L. Harris and M. T. Gladwin, *Nat. Chem. Biol.*, 2006, **2**, 486; (*c*) D. Fukumara, S. Kashiwagi and R. K. Jain, *Nat. Rev. Cancer*, 2006, **6**, 521; (*d*) N. Finney, *Nat. Chem. Biol.*, 2006, **2**, 349.
4 A. Webb, R. Bond, P. McLean, R. Uppal, N. Benjamin and A. Ahluwalia, *Proc. Natl. Acad. Sci. USA*, 2004, **101**, 13683.
5 A. Butler and R. Nicholson, in *Life, Death and Nitric Oxide*, Royal Society of Chemistry, Cambridge, 2003.
6 N. S. Bryan, T. Rassaf, R. E. Maloney, C. M. Rodriguez, F. Saijo, J. R. Rodriguez and M. Feelisch, *Proc. Natl. Acad. Sci. USA*, 2004, **101**, 4308.
7 *Data for Biochemical Research*, ed. R. M. C. Dawson, D. C. Elliot, W. H. Elliot and K. M. Jones, Oxford University Press, New York, 1969, pp. 438–439.
8 S. Bhaduri, N. S. Gupta, G. K. Lahiri and P. Mathur, *Organometallics*, 2004, **23**, 3733.
9 S. Bhaduri, P. Mathur, P. Payra and K. Sharma, *J. Am. Chem. Soc.*, 1998, **120**, 12127.
10 S. Bhaduri and K. Sharma, *J. Chem. Soc., Chem. Commun.*, 1992, **21**, 1593.
11 G. Longoni and P. Chini, *J. Am. Chem. Soc.*, 1976, **98**, 7225.
12 N. S. Gupta, P. Mathur, M. Doble and S. Bhaduri, *Inorg. Chim. Acta*, 2006, **359**, 3895.
13 A. Earnshaw, P. C. Hewlett and L. F. Larkworthy, *J. Chem. Soc.*, 1965, 4718.
14 (*a*) D. Zheng and R. L. Birke, *J. Am. Chem. Soc.*, 2001, **123**, 4637; (*b*) D. Zheng and R. L. Birke, *J. Am. Chem. Soc.*, 2002, **124**, 9066.
15 (*a*) B. O. Fernandez, I. M. Lorkovic and P. C. Ford, *Inorg. Chem.*, 2004, **43**, 5393; (*b*) A. K. Patra and P. K. Mascharak, *Inorg. Chem.*, 2003, **42**, 7363.
16 (*a*) D. Becke, *Phys. Rev. A*, 1988, **38**, 3098; (*b*) C. Lee, W. Yang and R. G. Parr, *Phys. Rev. B*, 1988, **37**, 785; (*c*) A. D. Becke, *J. Chem. Phys.*, 1993, **98**, 5648.
17 M. J. Frisch, G. W. Trucks, H. B. Schlegel, G. E. Scuseria, M. A. Robb, J. R. Cheeseman, V. G. Zakrzewski, J. A. Montgomery, Jr., R. E. Stratmann, J. C. Burant, S. Dapprich, J. M. Millam, A. D. Daniels, K. N. Kudin, M. C. Strain, O. Farkas, J. Tomasi, V. Barone, M. Cossi, R. Cammi, B. Mennucci, C. Pomelli, C. Adamo, S. Clifford, J. Ochterski, G. A. Petersson, P. Y. Ayala, Q. Cui, K. Morokuma, P. Salvador, J. J. Dannenberg, D. K. Malick, A. D. Rabuck, K. Raghavachari, J. B. Foresman, J. Cioslowski, J. V. Ortiz, A. G. Baboul, B. B. Stefanov, G. Liu, A. Liashenko, P. Piskorz, I. Komaromi, R. Gomperts, R. L. Martin, D. J. Fox, T. Keith, M. A. Al-Laham, C. Y. Peng, A. Nanayakkara, M. Challacombe, P. M. W. Gill, B. Johnson, W. Chen, M. W. Wong, J. L. Andres, C. Gonzalez, M. Head-Gordon, E. S. Replogle and J. A. Pople, *GAUSSIAN 98, Revision A.11*, Gaussian, Inc., Pittsburgh PA, 2001.

